Research Square

Preprints are preliminary reports that have not undergone peer review.
They should not be considered conclusive, used to inform clinical practice,
or referenced by the media as validated information.

Gelatin and PLG-based Scaffolds Differentially Support Follicle Integrity and Oocyte Growth in a 3D printed Scaffold

Vasiliki E Mourikes
Lurie Children's Hospital
Claire Joswiak
Lurie Children's Hospital
Sarah Palmer
Dimension Bio
Ramille N Shah
Dimension Bio
Monica M Laronda
mlaronda@luriechildrens.org

Lurie Children's Hospital

Research Article

Keywords: ovarian tissue engineering, follicle culture, bioprosthetic ovary, fertility preservation, biomaterials, ovarian follicle

Posted Date: November 4th, 2026

DOI: https://doi.org/10.21203/rs.3.rs-11394289/v1

License: This work is licensed under a Creative Commons Attribution 4.0 International License.
Read Full License

Additional Declarations: Competing interest reported. M.M.L. and R.N.S. are named inventors on U.S. Patent No. 10,479,980 B2, entitled “Artificial Ovary,” assigned to Northwestern University. R.N.S. is a current employee of Dimension Bio, and S.P. is a former employee. M.M.L., R.N.S., and S.P. have equity interests in Dimension Bio. The remaining authors declare no competing interests.

Abstract

Purpose

Life-saving cancer treatments can impair ovarian function, leaving many survivors, particularly children and adolescents, at risk of infertility, endocrine dysfunction, and premature menopause. Because transplantation of cryopreserved ovarian tissue is contraindicated in patients with ovarian malignancies, biomaterial-based strategies are needed to support isolated follicles within a bioprosthetic ovary.

Methods

We compared three 3D-printed scaffold materials for ovarian tissue engineering: ultra-fluffy poly(lactic-co-glycolic acid) (UF-PLG), gelatin, and gelatin-coated UF-PLG (UF-PLG-gel). Murine secondary follicles were cultured on each scaffold for 2, 4, or 6 days. Follicle adherence, structural integrity, stromal cell attachment, and oocyte growth were assessed by confocal microscopy. The effects of increased scaffold crosslinking on scaffold stiffness and follicle outcomes were also evaluated.

Results

Scaffold composition significantly influenced follicle behavior. Gelatin scaffolds promoted follicle retention and preserved follicular integrity, whereas UF-PLG scaffolds exhibited frequent follicle detachment and rupture. Oocytes cultured on UF-PLG-gel scaffolds achieved diameters associated with developmental competence. Increasing scaffold crosslinking altered scaffold stiffness but produced only modest effects on follicle morphology, attachment, and oocyte growth.

Conclusions

Scaffold composition is a major determinant of follicle behavior *in vitro*, and the biomaterial properties supporting follicle maintenance may differ from those promoting oocyte growth. Multi-material scaffold designs may therefore be required to better support the distinct requirements of follicle maintenance and maturation in future bioprosthetic ovaries.

Capsule Summary

Gelatin and PLG-based scaffolds differentially support follicle retention and oocyte growth during in vitro follicle culture, suggesting that distinct biomaterial properties may be required to optimize follicle maintenance and maturation in future bioprosthetic ovary designs.

Introduction

Life-saving cancer treatments are often gonadotoxic, leaving many survivors, including children and adolescents, at risk of impaired ovarian function. In patients treated before puberty, ovarian damage can prevent pubertal development, cause infertility, and lead to premature menopause [1]. Inadequate sex

steroid production later in life also increases the risk of skeletal and cardiovascular disease [2, 3]. Because prepubertal ovaries cannot produce eggs for cryopreservation, ovarian tissue cryopreservation (OTC) is currently the only fertility preservation option for these patients. OTC is typically initiated before or at the start of treatment and involves the surgical removal and cryopreservation of the ovarian cortex containing the primordial follicle pool [4]. At reproductive age, cryopreserved tissues may be transplanted into patients with the goal of restoring ovarian hormonal output and ovulation. While a child can be born after ovarian tissue transplantation in 25–31% of patients, transplantation of cryopreserved ovarian tissue has variable success, often based on the size of the tissue transplanted [5, 6]. Importantly, an ovarian tissue autotransplant from cryopreserved tissue is contraindicated in patients with metastatic disease to the ovary, highlighting the need for alternative strategies to restore long-term hormone function and fertility in these patients [7–9].

One promising alternative is the development of a bioprosthetic ovary that supports follicle growth and hormone production using engineered biomaterial scaffolds that support isolated follicles through differentiation and ovulation. Follicles are highly dynamic structures that undergo substantial increases in size throughout folliculogenesis [10]. During this process, follicles depend on interactions with surrounding stromal cells and extracellular matrix for structural support and biochemical signaling. These interactions regulate granulosa cell behavior, follicle architecture, and oocyte development. Disruption of the follicular microenvironment can impair follicle growth and reduce oocyte quality, highlighting the importance of recreating both the biochemical and mechanical features of the native ovary [11–13].

Various biomaterials have been investigated for their ability to support ovarian follicles in vitro and in vivo [14–16]. The challenge lies in preserving the follicle's three-dimensional architecture while recapitulating the dynamic microenvironment of the ovary. This is particularly important for pediatric patients because their ovaries contain predominantly primordial follicles that must undergo extensive growth and maturation before producing a fertilizable egg. Biomaterial scaffolds may offer a way to support healthy follicles in patients with ovarian metastases by replacing diseased stromal tissue with an engineered microenvironment. Biomaterial scaffolds may offer a way to support healthy follicles in patients with ovarian metastases by replacing diseased stromal tissue with an engineered microenvironment.

The development of a bioprosthetic ovary by Laronda et al. represented a major advance in ovarian tissue engineering [13]. Using 3D-printed gelatin scaffolds, the authors demonstrated that scaffold geometry plays a critical role in supporting ovarian follicles. The microporous scaffolds were designed with advancing 60-degree angle between layers, creating corners that physically support spherical follicles while maintaining sufficient porosity for vascularization and tissue integration following transplantation [13]. Subsequent studies have demonstrated that the mechanical, architectural, and biochemical properties of biomaterials can significantly influence cell attachment, migration, proliferation, and differentiation[16–19].

Mechanical signaling is increasingly recognized as a key regulator of ovarian function. The ovary is mechanically heterogeneous, with the collagen-rich cortex exhibiting greater stiffness than the softer medulla [20]. This mechanical gradient is thought to contribute to the spatial organization of quiescent and growing follicles within the ovary [20]. Changes in extracellular matrix composition, tissue stiffness, and force transmission have been implicated in follicle activation, growth, and hormone production [20–27]. As follicles enlarge, they must continuously remodel and interact with their surrounding environment, suggesting that scaffold composition and mechanics may independently influence follicle retention, stromal cell migration, and oocyte development[13, 16, 28].

While scaffold geometry has been shown to support follicle architecture, less is known about how scaffold composition influences follicle-scaffold interactions and follicle development. Gelatin is a collagen-derived biomaterial that contains native extracellular matrix binding motifs capable of promoting cell attachment and migration. In contrast, synthetic polymers such as poly(lactic-co-glycolic acid) (PLG) offer tunable mechanical properties, controlled degradation, and excellent surgical handling characteristics but may interact differently with ovarian cells. Ultra-Fluffy PLG (UF-PLG) is a highly porous 3D-printed PLG biomaterial that exhibits approximately 94% porosity and can absorb more than eight times its weight in liquid or hydrogel [29]. The resulting nano- and micro-scale architecture resembles soft tissue extracellular matrix and supports cellular infiltration, making it an attractive candidate for ovarian tissue engineering applications.

In this study, we sought to further refine the bioprosthetic ovary by comparing UF-PLG, gelatin, and gelatin-coated UF-PLG scaffolds while maintaining the 60-degree advancing angle design established by Laronda et al. [13]. We evaluated follicle attachment, follicle integrity, stromal cell migration, and oocyte growth as indicators of scaffold performance. Because scaffold stiffness is also known to influence cellular behavior, we further examined whether increasing scaffold crosslinking altered follicle behavior outcomes. We hypothesized that scaffold composition would differentially regulate follicle retention and follicle growth, reflecting distinct material requirements for maintaining follicle architecture versus supporting oocyte maturation. Specifically, we anticipated that biomaterials that best support follicle attachment and stromal integration would not necessarily be the same biomaterials that most effectively support oocyte growth, highlighting the need to separately optimize these functions when designing next-generation bioprosthetic ovaries.

Methods

Preparing PLG-based scaffolds

UF-PLG scaffolds were prepared as previously described [29] by dissolving PLG (Evonik, 824S) in Dichloromethane, and adding ethyl glycol butyl ether, triacetin, and sieved copper sulfate (325 mesh, ~ 80:20 v/v copper sulfate:PLG) to the slurry. The slurry was vortexed for about 2 hours to ensure homogeneity. The UF-PLG slurry printed at room temperature using an EnvisionTEC 3D BioPlotter and a 25-gauge tip (Nordson 7018391) at a pressure of 3–4 bar and a speed of 40–50 mm/s. Five layers of UF-

PLG were printed in a 5 cm x 5 cm square onto a frosted glass substrate. All layers were printed consisting of struts spaced 600 um apart (center to center distance) with the direction of the parallel struts advancing 60 deg every layer. The scaffolds were then washed in 70% EtOH and sterile DI water to dissolve and remove the copper sulfate particles, leaving behind the porous UF-PLG scaffold. The scaffolds were then frozen at -80C and lyophilized overnight.

After lyophilization, a portion of the UF-PLG scaffolds were washed in 70% EtOH and water and then placed into a 10% gelatin solution for 10 minutes and crosslinked in EDC/NHS 1x solution for 1 hour. The scaffolds were then washed with water once more, frozen at -80C and lyophilized, to create gelatin-coated UF-PLG scaffolds.

Preparing the Gelatin Scaffold

All scaffolds were also printed using the EnvisionTEC 3D BioPlotter. The day before printing, 10% gelatin solution was prepared by dissolving porcine skin gelatin (Sigma-Aldrich G1890) in 1X PBS. To ensure a homogenous solution, the gelatin was placed in a 35°C bead bath for 30 minutes, then vortexed thoroughly. After vortexing three times, the solution was centrifuged to remove air bubbles and transferred to a 30cc syringe barrel (Nordson EFD 7366054) and equilibrated to 30°C overnight in the print head.

Gelatin solution was extruded through a 27G blunt-tipped needle (Nordson EFD 7018395) with a pressure of 1–2 bar and a speed of 40–50 mm/s. Gelatin scaffolds were printed with the print head temperature set to 30°C and the platform temperature set to 4°C. Five layers of gelatin were printed onto a glass slide in a long (12 x 36 mm) rectangle. The first layer was printed with minimal distance between struts to create a solid bottom layer; all following layers consisted of struts spaced 600 μm apart (center-to-center distance), with the direction of the struts advancing 60° every layer. This resulted in struts 250 μm wide with an edge-to-edge distance of 350 μm (SI Fig. 1).

After scaffold printing was complete, the slides were kept in a humidity chamber on ice to avoid drying or melting of the gelatin. Structures were crosslinked for 1 hour with N-(3-dimethylaminopropyl)-N0-ethylcarbodiimide (EDC; Sigma-Aldrich) and N-hydroxysuccinimide (NHS; Sigma-Aldrich) solution in cold PBS at 4°C. 1X crosslinking solution consisted of 15 mM EDC and 6 mM NHS; 2X crosslinking used 30 mM EDC and 12 mM NHS. Scaffolds were then washed three times in deionized water and stored in 70% ethanol at 4°C until use.

On the day of culture, gelatin scaffolds were moved to sterile PBS and sterilized by 1 hour of UV exposure. To rehydrate the scaffolds, lyophilized PLG and UF-PLG prints were placed in 70% ethanol followed by sterile deionized water. All scaffolds were cut into discs using a 3 mm sterile biopsy punch; the punches were inspected under the dissecting scope to ensure quality, then equilibrated in follicle growth media (FGM, recipe below) at 37°C with 5% CO_2.

Mechanical Testing

To determine the stiffness of the printed scaffolds, indentation testing was performed using a Mach-01 V500C (Biomomentum MA001) with a 1.5 N load cell (Biomomentum MA999) and a 3 mm diameter plane-ended cylindrical indenter (Biomomentum MA463). Prior to testing, the indenter was positioned at the surface of the scaffold using the “Find contact” function with a force cutoff of 0.075 gf. Subsequently, the scaffold was indented to a depth of 250–500 μm over a period of 1 second. The resulting force-position curve was used in the Mach-01 Analysis software (Biomomentum SW186) to calculate the Young’s Modulus of the scaffold.

Follicle Culture

Culture media were prepared prior to each experiment. Dissection media (DM) consisted of L-15 medium (Cytiva SH30525.01) with 1% charcoal stripped fetal bovine serum (csFBS, Sigma-Aldrich F6765) and antibiotic-antimycotic solution (R&D Systems B22110). Maintenance media (MM) consisted of MEMα + GlutaMAX™ (Fisher Scientific 32-561-037) with 1% csFBS and antibiotic-antimycotic solution. Follicle growth media (FGM) consisted of MEMα + GlutaMAX™ with 3 mg/ml bovine serum albumin (BSA, Sigma-Aldrich A9418), bovine fetuin (Sigma-Aldrich F2379), 5 μg/ml insulin, 5 μg/ml transferrin and 5 ng/ml selenium (Sigma-Aldrich, I1884), antibiotic-antimycotic solution, and 10 mIU/ml follicle stimulating hormone (EMD Serono GONAL-f).

For each culture experiment, ovaries were isolated from 6–8 female CD1 mice (Charles River Labs) at 14–16 days postpartum and placed in DM. Under a dissecting microscope, ovaries were removed from the bursa and follicles were mechanically isolated using insulin syringes. Secondary follicles 150–180 μm in diameter were selected for culture and equilibrated in MM for 1 hour.

24-well plates were prepared with 400 μL of FGM and one transwell culture insert (Milicel PICM01250) with a 3 mm scaffold punch per well (Fig. 1). One secondary follicle was seeded onto each scaffold and positioned near an intersection of struts to allow for maximum contact with the scaffold (SI Fig. 2). Follicles were assigned to scaffold type and collection time point, with separate follicles analyzed after 2, 4, or 6 days of culture. Approximately 10 follicles per scaffold type were assigned to each time point for the scaffold-composition experiments. For the crosslinking experiments, three independent culture experiments were performed for each scaffold material and data were pooled across experiments. The number of follicles included in individual analyses varied because detached or unrecoverable follicles could not be assessed for scaffold attachment, and oocyte diameter could only be measured when an oocyte was clearly visible. Follicles were cultured for 6 days at 37°C and 5% CO_2. Half the volume of the culture media was replaced every other day. At each designated collection time point (days 2, 4, and 6), the corresponding cohort of follicles was removed from culture and fixed with 4% paraformaldehyde (PFA) through the transwell membrane. After fixing for 20 minutes at room temperature, the transwells were moved to PBS with 0.1% Tween-20 (PBS-T). To better investigate the follicle-scaffold interaction,

the scaffolds were embedded by carefully filling the transwells with 2% agarose. Once solidified, the agarose-embedded scaffolds were removed from the transwells and stored in PBS-T at 4°C.

Confocal Microscopy

Agarose-embedded scaffolds were incubated overnight at 4°C with Hoechst 33342 (Sigma Aldrich B2261) and phalloidin conjugated with AlexaFluor 488 (Thermo Fisher Scientific A12379) diluted in phosphate buffered saline (PBS). The scaffolds were then washed three times in PBS-T and imaged on a Zeiss LSM 880 Confocal Laser Scanning Microscope. Z-stacks were acquired using a 10x objective with a slice depth of 10 µm. Differential interference contrast (DIC) was used to visualize the scaffold during imaging without brightfield.

Follicle Adherence, Integrity and Attachment Analyses

Follicle adherence and integrity were determined by confocal microscopy. A follicle was considered detached if it could not be found within the confines of the scaffold or if it was observed between struts without any cellular attachments to the struts. Follicles that remained adhered were further categorized as being intact or ruptured. A follicle was considered intact if the basement membrane remained intact. Oocyte visibility was assessed separately. A follicle was considered ruptured if the basement membrane was disrupted and/or the oocyte was detected outside the boundary of the follicle basement membrane.

Area of follicle attachment to a scaffold was determined by confocal microscopy and analyzed in FIJI. Z-stacks were flattened into single frames using a maximum intensity Z-projection. For samples with visible oocytes, additional maximum intensity Z-projections were created from partway through the stack to allow for measurement of oocyte diameter. Phalloidin signal was used to measure attachment by creating a separate Z-projection of the green channel. Follicles were first manually circled and deleted from the projection. Then, the image was binarized using the threshold tool and the areas of positive phalloidin signal were measured (SI Fig. 3).

Statistical Analyses

Statistical Analyses were performed using GraphPad Prism. Data are presented as means ± SEM (standard error of the mean). Multiple comparisons between normally distributed experimental groups were made using one-way analysis of variance (ANOVA) or a Mixed Effects Model. If data were not normally distributed, comparisons between groups were made by Kruskal-Wallis test. Statistical significance was assigned at $p \leq 0.05$.

Results

Follicle adherence and integrity

To evaluate whether scaffold composition influences the ability of isolated follicles to remain attached and structurally intact during culture, follicle adherence and integrity were determined by confocal microscopy (Fig. 2a,c,e). Follicles cultured on UF-PLG scaffolds tended to fall off the scaffold or rupture. 78% of follicles detached from the UF-PLG scaffolds and 22% remained attached and intact after two days in culture (Fig. 2b). A smaller proportion of the follicles that were attached on day 2 became detached by days 4 or 6 of culture (20% and 30% respectively); however, approximately half of these attached follicles ruptured (Fig. 2b). Unlike the UF-PLG, most of the follicles cultured on UF-PLG-gel scaffolds remained adhered to the scaffold (Fig. 2c). All of the adhered follicles remained intact after two days of culture, but the proportion of ruptured follicles increased following four and six days. By day 6, 73% of follicles were ruptured (Fig. 2d). Nearly all (90%, 100%, 90% for days 2, 4, 6 of culture) the follicles cultured on gelatin scaffolds remained adhered, and all the adhered follicles remained intact (Fig. 2e and 2f).

Follicle attachment

To determine whether scaffold composition supports follicle integration with the scaffold over time, the degree of follicle attachment and stromal cell migration were determined by confocal microscopy (Fig. 3a,d,g). This is destructive sampling where the same follicle is not able to be measured over the culture period. Data are missing from the day 2 UF-PLG scaffold because nearly all follicles fell off the scaffold. The area of attachment between the follicles and the UF-PLG scaffold was approximately the same after 4 (20×10^3 mm^2) and 6 (25×10^3 mm^2) days in culture (Fig. 3b). This was also true of the average number of struts with stromal cell migration. There was an average of 1.8 struts on day 4 and 2.3 struts on day 6. (Fig. 3c). The area of attachment between the follicles and the UF-PLG-gel scaffolds incrementally increased, while the average number of struts with cell significantly increased on days 4 and 6 (2 struts) compared to day 2 (0.8 struts) (Fig. 3e and f). The area of attachment between the follicles and the gelatin scaffolds was significantly greater on days 4 (83.5×10^3 mm^2) and 6 (81.5×10^3 mm^2) compared to day 2 (5.2×10^3 mm^2) (Fig. 3h). Similarly, there was a significant increase in the average number of struts with adhered and migrated cells on days 4 (3.1 struts) and 6 (2.8 struts) compared to day 2 (0.7 struts) (Fig. 3i).

Oocyte diameter

To determine whether scaffold composition supports oocyte growth toward developmental competence, oocyte diameter within intact follicles was quantified by confocal microscopy (Fig. 4a). In mice, oocytes acquire developmental competence upon completing growth at a cytoplasmic diameter of approximately 70–72 μm, making oocyte diameter a commonly used surrogate measure of developmental competence[30, 31]. Data are missing from the day 2 UF-PLG scaffold because nearly all follicles fell off the scaffold. None of the oocytes cultured on UF-PLG or gelatin scaffolds reached the 72 μm benchmark of oocyte competence (Fig. 4b and d). The oocytes cultured on the UF-PLG-gel scaffold for 6 days were the only group to surpass the competence benchmark averaging 75.6 μm (Fig. 4c). Overall, the oocytes cultured on the gelatin scaffolds were smaller than those cultured on the PLG-containing scaffolds.

Effects of scaffold crosslinking

To determine whether increasing scaffold crosslinking influences follicle morphology, scaffold mechanics, follicle attachment, and oocyte growth, follicles were cultured on UF-PLG-gel and gelatin scaffolds crosslinked with either 1x or 2x concentrations of crosslinking reagent and evaluated qualitatively and quantitatively (Figs. 5 and 6). Representative confocal images illustrate the morphological categories used to classify follicles cultured on UF-PLG-gel (Fig. 5a) and gelatin (Fig. 5b) scaffolds. Follicles were categorized based on attachment, follicle integrity, and oocyte visibility. Across both scaffold types, the proportion of intact follicles generally decreased with time in culture, accompanied by an increase in follicle rupture. Follicle detachment was observed more frequently on 1x crosslinked scaffolds, whereas follicles cultured on 2x crosslinked scaffolds, made of either UF-PLG-gel or gelatin, generally remained associated with the scaffold throughout culture. These trends were observed for both UF-PLG-gel and gelatin scaffolds, although the distribution of follicle morphology varied with scaffold composition, degree of crosslinking, and time in culture (Fig. 5c-f).

To determine whether these qualitative differences were associated with changes in scaffold mechanics, scaffold stiffness was measured by indentation testing. Increasing the concentration of crosslinking reagent significantly increased the Young's modulus of gelatin scaffolds from 7.2 kPa to 22.8 kPa (Fig. 6b), whereas no significant difference was observed between 1x and 2x UF-PLG-gel scaffolds (16.1 kPa vs. 25.4 kPa) (Fig. 6a).

To determine whether altered scaffold mechanics influenced follicle-scaffold interactions, the area of follicle attachment was quantified. For UF-PLG-gel scaffolds, the area of attachment measured 20.2 mm^2, 74.4 mm^2, and 121.0 mm^2 on days 2, 4, and 6, respectively, in the 1x crosslinked group compared with 8.2 mm^2, 32.7 mm^2, and 62.7 mm^2 in the 2x crosslinked group (Fig. 6c). Similarly, the area of attachment for gelatin scaffolds measured 52.3 x 10^3 mm^2, 180.5 x 10^3 mm^2, and 208.6 x 10^3 mm^2 on days 2, 4, and 6 in the 1x crosslinked group compared with 95.6 x 10^3 mm^2, 182.8 x 10^3 mm^2, and 309.7 x 10^3 mm^2 in the 2x crosslinked group (Fig. 6d).

Finally, to determine whether increasing scaffold crosslinking altered follicle growth, oocyte diameter was quantified within intact follicles. Increased crosslinking did not affect oocyte diameter in the UF-PLG-gel scaffold (Fig. 6e) or the gelatin scaffold (Fig. 6f). Overall, increasing scaffold crosslinking altered the mechanical properties of gelatin scaffolds but had only modest effects on follicle morphology, follicle attachment, and oocyte growth.

Discussion

We directly compared PLG formulations that have successfully supported other types of tissue development, with gelatin that was previously used in bioprosthetic ovary transplants in mice [13, 29, 32]. PLG is easier to print, making reproducibility more reliable, has a more stable shelf-life and is easier to handle (and therefore transplant) compared to gelatin. Additionally, printed ultra-fluffy or fluffy-PLGs

have tunable porous struts that could allow for the addition of gelatin or other ECM-based hydrogels to promote cell attachment. Therefore, to determine if this material could support a bioprosthetic ovary transplant, we directly compared scaffolds generated from UF-PLG and UF-PLG-gel directly with the gelatin scaffold printed in the same design that supported follicle cultures in a previous study (60° advancing-angle architecture). Additionally, we performed these experiments using isolated secondary murine follicles and calculated the parameters that were shown to be correlated with success in previous bioprosthetic ovary experiments that produced live pups as transplants [13]. We compared three biomaterial scaffolds and found that scaffold composition had an impact on follicle behavior, influencing follicle attachment, structural integrity, stromal cell migration, and oocyte growth. Gelatin scaffolds consistently supported follicle attachment and maintained follicular integrity throughout the culture period, whereas follicles cultured on UF-PLG scaffolds frequently detached from the scaffold or ruptured. Interestingly, the scaffold that best supported follicle retention was not the scaffold that best supported oocyte growth. Oocytes cultured on UF-PLG-gel scaffolds achieved diameters associated with oocyte competence, whereas oocytes cultured on gelatin scaffolds remained comparatively smaller. Together, these findings suggest that the biomaterial properties required to maintain follicle architecture may differ from those required to support oocyte growth, highlighting an important design consideration for future ovarian tissue engineering strategies.

Successful follicle culture requires maintenance of the three-dimensional relationship between the oocyte, granulosa cells, and surrounding stromal cells. Once a follicle detaches from the scaffold, it loses the physical support necessary to maintain its architecture and becomes susceptible to rupture. The extensive stromal cell migration observed throughout the gelatin scaffolds likely contributed to the improved retention of follicles by increasing the area of contact between the follicle and scaffold and distributing mechanical forces across multiple attachment sites. This behavior is consistent with the biological properties of gelatin, a collagen-derived biomaterial that contains native extracellular matrix adhesion motifs capable of promoting integrin-mediated cell attachment, migration, and remodeling [33–35]. In contrast, PLG-based materials are comparatively bioinert and may require surface modification to enhance cell adhesion [36, 37]. The reduced attachment observed on UF-PLG scaffolds may therefore reflect an inability of stromal cells to establish sufficient scaffold interactions during the early stages of culture.

The differences observed between scaffold materials likely extend beyond cellular adhesion alone. Biomaterials influence a wide range of physical and biochemical signals that collectively shape cell behavior. Gelatin readily hydrates and swells in aqueous environments, facilitating rapid media penetration and cellular infiltration, whereas PLG-based materials exhibit distinct degradation characteristics, surface chemistries, and mechanical properties. These differences may alter nutrient diffusion, extracellular matrix deposition, mechanotransduction pathways, and the ability of stromal cells to remodel their microenvironment. Because follicle development depends on continuous communication between granulosa cells, stromal cells, and the oocyte, even subtle differences in the local microenvironment may produce substantial effects on follicle behavior over time.

Despite the superior follicle retention observed in gelatin scaffolds, oocyte growth appeared more favorable within PLG-containing scaffolds. Only follicles cultured on UF-PLG-gel scaffolds achieved oocyte diameters associated with developmental competence during the culture period. Although the mechanism underlying this observation remains unclear, the finding suggests that the scaffold properties that promote follicle attachment are not necessarily the same properties that support oocyte growth. Previous studies, reviewed extensively by Fiorentino et al., have demonstrated that follicle development is regulated not only by biochemical signaling but also by physical forces generated within the follicle and transmitted through the surrounding extracellular matrix [38]. The more permissive architecture of PLG-containing scaffolds may provide an environment that better accommodates follicle expansion and growth, whereas the strong adhesive interactions observed within gelatin scaffolds may constrain follicular remodeling. Alternatively, differences in nutrient transport, matrix remodeling, or mechanical stress distribution may contribute to the divergent developmental outcomes observed between scaffold materials. Importantly, the present study was not designed to distinguish among these possibilities, and additional mechanistic studies will be required to identify the specific scaffold properties responsible for promoting oocyte growth.

To further investigate the role of mechanics, we evaluated the effects of increased scaffold crosslinking. Crosslinking increased scaffold stiffness but produced relatively modest changes in follicle attachment and oocyte growth compared with the differences observed between biomaterial compositions. These findings suggest that scaffold composition may exert a greater influence on follicle behavior than stiffness alone within the range of mechanical properties examined in this study. This observation is notable given the growing appreciation for the role of mechanobiology in regulating ovarian function. The ovary contains mechanically distinct cortical and medullary compartments, and emerging evidence suggests that tissue stiffness influences follicle activation, growth, and hormone production [38, 39] [20] [40, 41]. While our findings do not exclude an important role for mechanics, they indicate that the biological and physicochemical characteristics of the scaffold material itself may be equally important determinants of follicle behavior.

The apparent divergence between follicle retention and oocyte growth has important implications for the design of future bioprosthetic ovaries. Historically, scaffold development has often focused on identifying a single biomaterial capable of supporting all aspects of follicle development. Our findings suggest that different scaffold properties may be required to support distinct biological functions. The native ovary itself is not mechanically uniform. Quiescent follicles reside within the relatively stiff cortex, whereas growing follicles are located within the softer and more permissive medulla [20]. This compartmentalized organization likely reflects the differing biological requirements of follicle maintenance and follicle growth. The observation that gelatin scaffolds favored follicle retention while PLG-containing scaffolds favored oocyte growth suggests that future ovarian constructs may benefit from incorporating multiple biomaterials that mimic these distinct ovarian compartments. Multi-material printing technologies and spatially controlled biomaterial architectures may ultimately allow the creation of engineered ovaries that support both long-term follicle maintenance and continued follicle maturation.

In conclusion, scaffold composition significantly influenced follicle attachment, structural integrity, and oocyte growth in cultured murine secondary follicles. Gelatin scaffolds promoted extensive stromal cell migration and supported long-term follicle retention, whereas PLG-containing scaffolds appeared more favorable for oocyte growth. Manipulation of scaffold stiffness alone produced comparatively modest effects, suggesting that material composition plays a dominant role in shaping follicle behavior within these culture systems. Collectively, these findings demonstrate that the scaffold properties required to support follicle maintenance may differ from those required to support follicle maturation and provide a framework for the development of next-generation bioprosthetic ovaries that incorporate distinct microenvironments optimized for different stages of folliculogenesis.

Declarations

Competing Interests

M.M.L. and R.N.S. are named inventors on U.S. Patent No. 10,479,980 B2, entitled “Artificial Ovary,” assigned to Northwestern University. R.N.S. is a current employee of Dimension Bio, and S.P. is a former employee. M.M.L., R.N.S., and S.P. have equity interests in Dimension Bio. The remaining authors declare no competing interests.

Author Contribution

Material preparation, data collection, and analysis were performed by V.E.M., C.J., and S.P. under the guidance and supervision of R.N.S. and M.M.L. The first draft of the manuscript was written by V.E.M. and edited by M.M.L. All authors commented and edited on subsequent versions of the manuscript. All authors read and approved the final manuscript.

Acknowledgement

Acknowledgements: The authors would like to thank the Histology and Microscopy Group at the Stanley Manne Children’s Research Institute, affiliated with Ann & Robert H. Lurie Children’s Hospital of Chicago.

Data Availability

Data Availability Statement: The datasets generated and/or analyzed during the current study are available from the corresponding author on reasonable request.

References

1. Anazodo A, et al. Oncofertility-An emerging discipline rather than a special consideration. Pediatr Blood Cancer. 2018;65(11):e27297.

2. Hodis HN, Mack WJ. Menopausal Hormone Replacement Therapy and Reduction of All-Cause Mortality and Cardiovascular Disease: It Is About Time and Timing. Cancer J. 2022;28(3):208–23.
3. Ryczkowska K, et al. Menopause and women's cardiovascular health: is it really an obvious relationship? Arch Med Sci. 2023;19(2):458–66.
4. Chakravarthy R, Laronda MM, Zarnegar-Lumley S. Oncofertility in Pediatric and Adolescent Patients: Current Practice and Future Directions. Hematol Oncol Clin North Am. 2026;40(3):379–91.
5. Diaz AA, et al. A Systematic Review of Ovarian Tissue Transplantation Outcomes by Ovarian Tissue Processing Size for Cryopreservation. Front Endocrinol (Lausanne). 2022;13:918899.
6. Erden M, et al. Perinatal outcomes of pregnancies following autologous cryopreserved ovarian tissue transplantation: a systematic review with pooled analysis. Am J Obstet Gynecol. 2024;231(5):480–9.
7. Jeruss JS, Woodruff TK. Preservation of fertility in patients with cancer. N Engl J Med. 2009;360(9):902–11.
8. Boudry A, et al. Assessment of measurable residual disease in ovarian tissue collected for fertility preservation in patients in remission from acute myeloid leukaemia: A pilot study. Br J Haematol. 2026;208(3):897–904.
9. Laronda MM, et al. Initiation of puberty in mice following decellularized ovary transplant. Biomaterials. 2015;50:20–9.
10. Gougeon A. Human ovarian follicular development: from activation of resting follicles to preovulatory maturation. Ann Endocrinol (Paris). 2010;71(3):132–43.
11. Hornick JE, et al. Isolated primate primordial follicles require a rigid physical environment to survive and grow in vitro. Hum Reprod. 2012;27(6):1801–10.
12. Laronda MM, et al. Alginate encapsulation supports the growth and differentiation of human primordial follicles within ovarian cortical tissue. J Assist Reprod Genet. 2014;31(8):1013–28.
13. Laronda MM, et al. A bioprosthetic ovary created using 3D printed microporous scaffolds restores ovarian function in sterilized mice. Nat Commun. 2017;8:15261.
14. Shea LD, Woodruff TK, Shikanov A. Bioengineering the ovarian follicle microenvironment. Annu Rev Biomed Eng. 2014;16:29–52.
15. West ER, Shea LD, Woodruff TK. Engineering the follicle microenvironment. Semin Reprod Med. 2007;25(4):287–99.
16. Henning NFC, Jakus AE, Laronda MM. Building Organs Using Tissue-Specific Microenvironments: Perspectives from a Bioprosthetic Ovary. Trends Biotechnol. 2021;39(8):824–37.
17. Shellard A, Mayor R. All Roads Lead to Directional Cell Migration. Trends Cell Biol. 2020;30(11):852–68.
18. Yao B, et al. Biochemical and structural cues of 3D-printed matrix synergistically direct MSC differentiation for functional sweat gland regeneration. Sci Adv. 2020;6(10):eaaz1094.

19. Beaune G, et al. Spontaneous migration of cellular aggregates from giant keratocytes to running spheroids. Proc Natl Acad Sci U S A. 2018;115(51):12926–31.
20. Tsui EL, et al. Human ovarian gross morphology and subanatomy across puberty: insights from tissue donated during fertility preservation. F S Rep. 2023;4(2):196–205.
21. McDowell HB, Henning NF, Laronda MM. Heterogeneity of ovarian matrisome hydrogels elucidates factors that may influence follicle growth in vitro. Reproduction, 2024. 168(3).
22. McDowell HB et al. Generation of Tailored Extracellular Matrix Hydrogels for the Study of In Vitro Folliculogenesis in Response to Matrisome-Dependent Biochemical Cues. Bioeng (Basel), 2024. 11(6).
23. Nagamatsu G, et al. The intrinsic impact of mechanical stress on the maintenance of oocyte dormancy. Proc Natl Acad Sci U S A. 2026;123(3):e2526249123.
24. Nagamatsu G, et al. Mechanical stress accompanied with nuclear rotation is involved in the dormant state of mouse oocytes. Sci Adv. 2019;5(6):eaav9960.
25. McElhinney KL, Rowell EE, Laronda MM. *Encapsulation of Bovine Primordial Follicles in Rigid Alginate Does Not Affect Growth Dynamics.* Bioengineering (Basel), 2024. 11(7).
26. West ER, et al. Physical properties of alginate hydrogels and their effects on in vitro follicle development. Biomaterials. 2007;28(30):4439–48.
27. Ouni E, et al. A blueprint of the topology and mechanics of the human ovary for next-generation bioengineering and diagnosis. Nat Commun. 2021;12(1):5603.
28. Shikanov A, et al. Hydrogel network design using multifunctional macromers to coordinate tissue maturation in ovarian follicle culture. Biomaterials. 2011;32(10):2524–31.
29. Jakus AE, et al. 3D-printing porosity: A new approach to creating elevated porosity materials and structures. Acta Biomater. 2018;72:94–109.
30. Eppig JJ, O'Brien MJ. Development in vitro of mouse oocytes from primordial follicles. Biol Reprod. 1996;54(1):197–207.
31. Eppig JJ, et al. Factors affecting the developmental competence of mouse oocytes grown in vitro: follicle-stimulating hormone and insulin. Biol Reprod. 1998;59(6):1445–53.
32. Yan B et al. Surface Modification Progress for PLGA-Based Cell Scaffolds. Polym (Basel), 2024. 16(1).
33. Echave MC, et al. Gelatin as Biomaterial for Tissue Engineering. Curr Pharm Des. 2017;23(24):3567–84.
34. Lukin I et al. Progress in Gelatin as Biomaterial for Tissue Engineering. Pharmaceutics, 2022. 14(6).
35. Tang-Quan KR, et al. Gelatin Promotes Cell Retention Within Decellularized Heart Extracellular Matrix Vasculature and Parenchyma. Cell Mol Bioeng. 2020;13(6):633–45.
36. Tryba AM, et al. Surface Functionalization of Poly(l-lactide-co-glycolide) Membranes with RGD-Grafted Poly(2-oxazoline) for Periodontal Tissue Engineering. J Funct Biomaterials. 2022;13(1):4.

37. Guerriero I, et al. Programming Degradation and Drug Release Through Micropatterning of PLGA Films. ACS Appl Mater Interfaces. 2026;18(20):28464–78.
38. Fiorentino G, et al. Biomechanical forces and signals operating in the ovary during folliculogenesis and their dysregulation: implications for fertility. Hum Reprod Update. 2023;29(1):1–23.
39. HaiYang W, et al. Mechanopharmacology of cellular microenvironment stiffness: Therapeutic strategies for age-related diseases. Br J Pharmacol. 2026;183(4):945–56.
40. Amargant F, et al. Ovarian stiffness increases with age in the mammalian ovary and depends on collagen and hyaluronan matrices. Aging Cell. 2020;19(11):e13259.
41. Ouni E, et al. Spatiotemporal changes in mechanical matrisome components of the human ovary from prepuberty to menopause. Hum Reprod. 2020;35(6):1391–410.

Figures

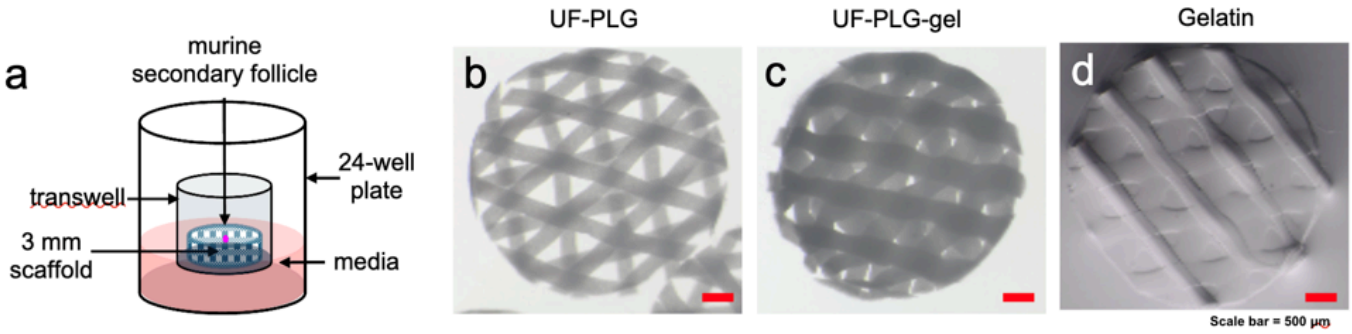


Figure 1

Culture system and scaffold architecture. (a) Schematic of culture system showing the placement of a scaffold on top of a trans well that is submerged in media. (b-d) UF-PLG, UF-PLG-gel, and Gelatin scaffolds imaged by light microscopy. Murine secondary follicles were placed within the scaffolds where three struts (red arrows) meet to create a 60° angle. Scale Bar = 500 µm

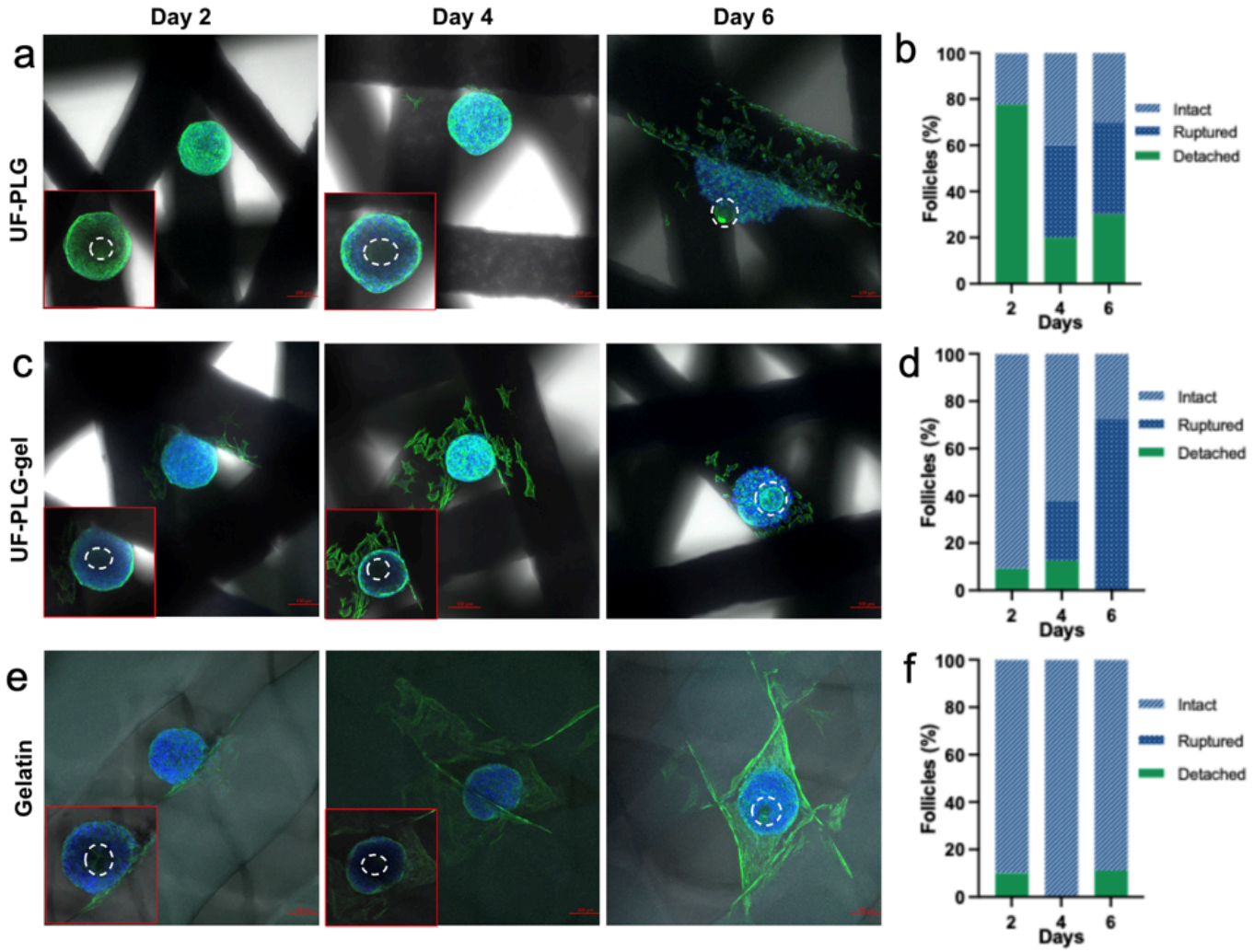


Figure 2

Follicle adherence and integrity. (a, c, e) Murine secondary follicles were cultured on scaffolds made of UF-PLG, UF-PLG-gel, or gelatin for 2, 4, or 6 days. Representative images show follicles situated between three scaffold struts (white arrows) which meet to create a 60° angle. Insets show deeper z-planes of the follicles where oocytes are visible (white dashed circle). (b, d, f) Follicles were categorized based on attachment and integrity. Follicles that detached from scaffolds are represented by solid green bars. Follicles that remained attached to the scaffold were subcategorized based on whether they were intact (lined blue bars) or ruptured (dotted blue bars).

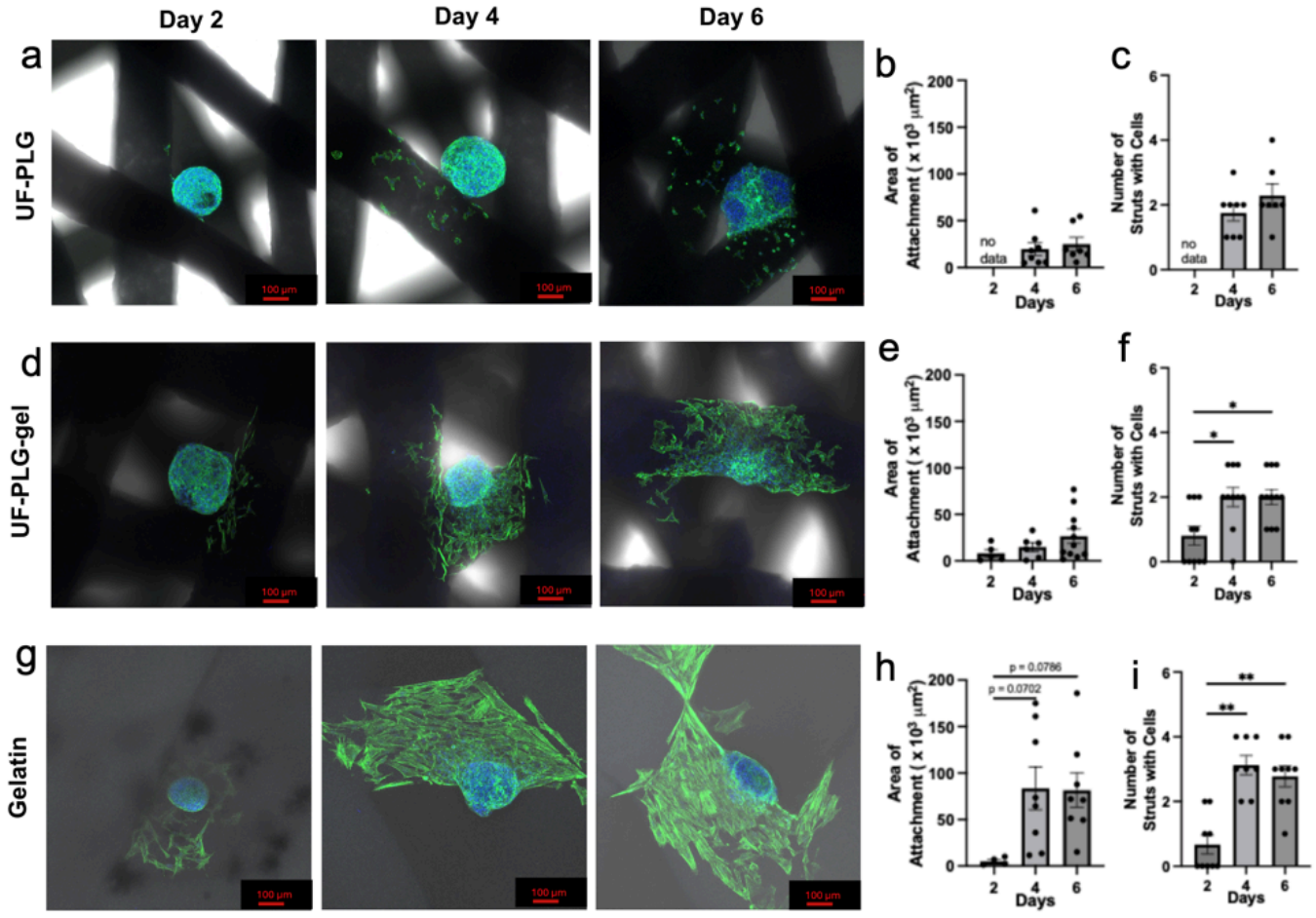


Figure 3

Follicle attachment: (a, d, g) Murine secondary follicles were cultured on scaffolds made of UF-PLG, UF-PLG-gel, or gelatin for 2, 4, or 6 days. Representative images show contact area between follicle and scaffold struts. Struts are indicated by white arrows.

The area of attachment and the number of struts with cells were quantified for follicles cultured on UF-PLG(b & c), UF-PLG-gel (e & f), and gelatin(h & i) scaffolds. Data are missing from the day 2 UF-PLG scaffold because nearly all follicles fell off the scaffold. Graphs depict means ± SEM. Asterisks indicate significant differences between culture time points. *P < 0.05, **P < 0.01

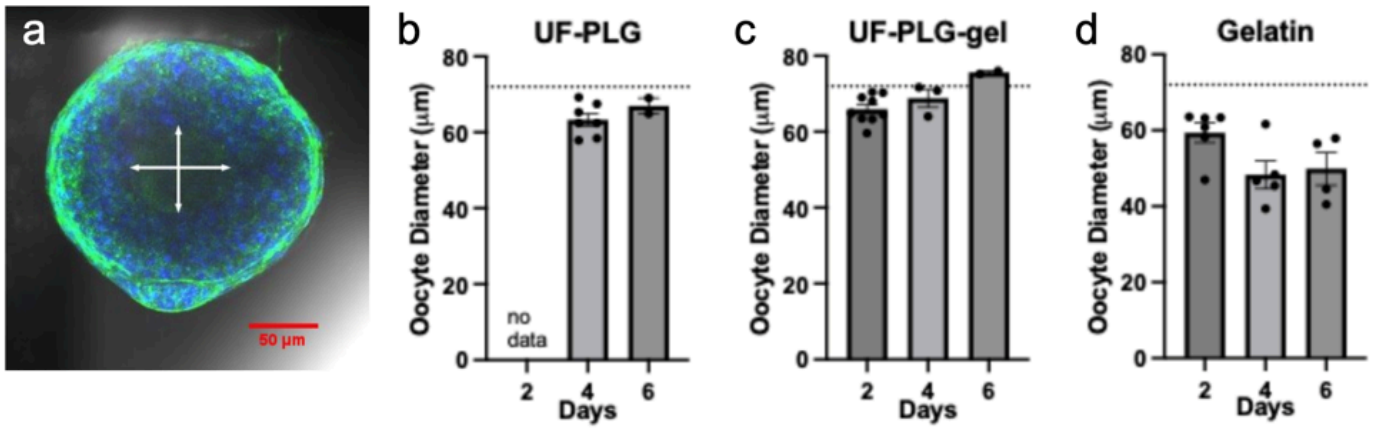


Figure 4

Oocyte diameter during scaffold culture. Murine secondary follicles were cultured on UF-PLG, UF-PLG-gel, or gelatin scaffolds for 2, 4, or 6 days. (a) Representative confocal image showing measurement of oocyte diameter within an intact follicle; white arrows indicate the oocyte boundaries used for measurement. Oocyte diameter was quantified for follicles cultured on (b) UF-PLG, (c) UF-PLG-gel, and (d) gelatin scaffolds. The dashed horizontal line at 72 µm indicates the approximate oocyte diameter associated with developmental competence in mice. Data are unavailable for day 2 UF-PLG because nearly all follicles detached from the scaffold. Graphs depict mean ± SEM.

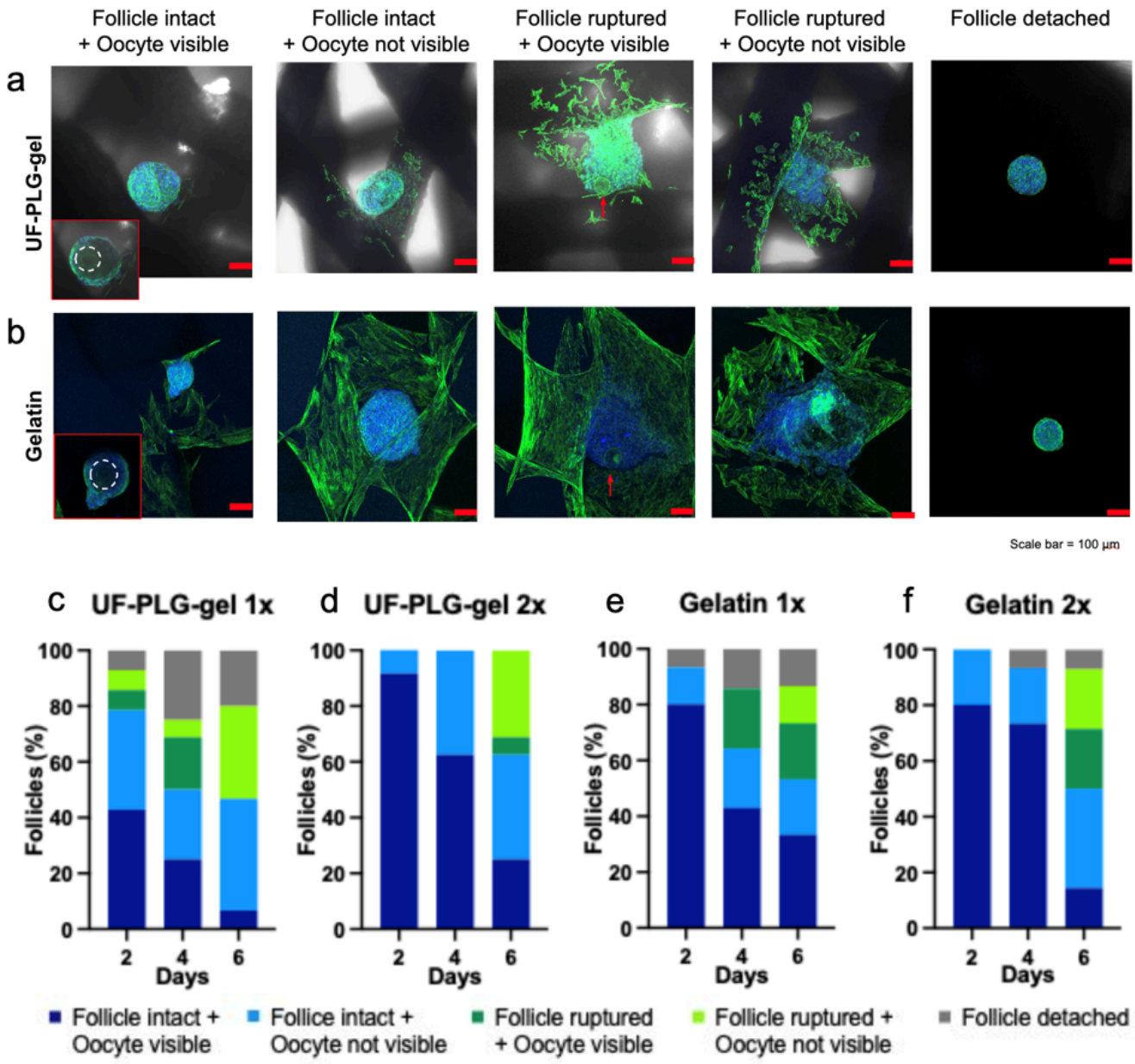


Figure 5

Effects of scaffold crosslinking on follicle and oocyte morphology. Murine secondary follicles were cultured on UF-PLG-gel or gelatin scaffolds crosslinked with either 1× or 2× concentrations of crosslinking reagent for 2, 4, or 6 days. Representative confocal images of follicles cultured on (a) UF-PLG-gel and (b) gelatin scaffolds illustrate the morphological categories used for classification based on scaffold attachment, follicle integrity, and oocyte visibility. Follicles were classified as detached, intact with a visible oocyte, ruptured with a visible oocyte, intact without a visible oocyte, or ruptured without a visible oocyte. Stacked bar graphs show the percentage of follicles in each category for (c) 1× crosslinked UF-PLG-gel, (d) 2× crosslinked UF-PLG-gel, (e) 1× crosslinked gelatin, and (f) 2× crosslinked

gelatin scaffolds. Red arrows indicate extruded oocytes, and insets show deeper z-planes in which oocytes are visible (white dashed circles). Scale bar = 100 μm.

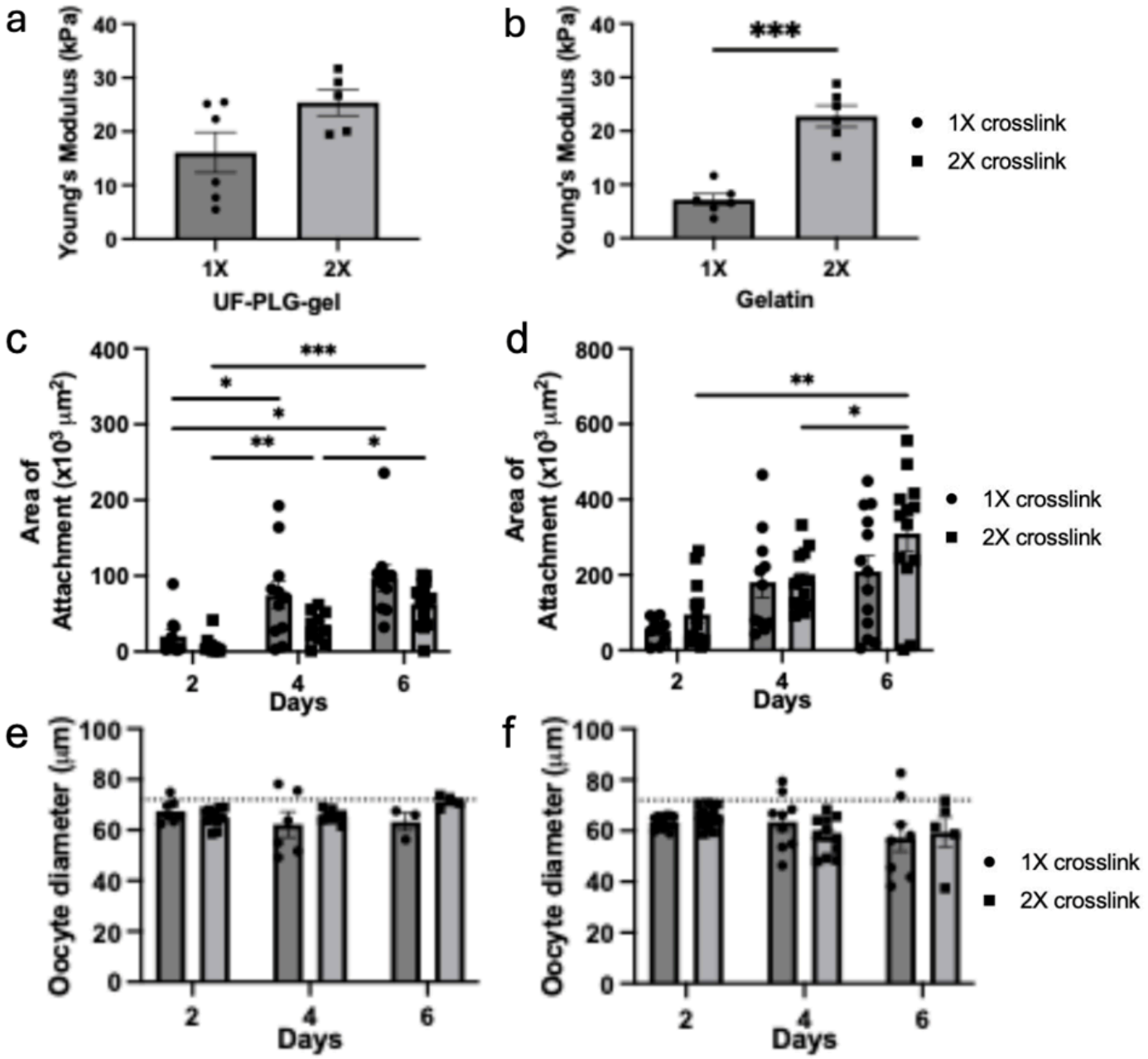


Figure 6

The effects of crosslinking on scaffold mechanics and follicle outcomes. Murine secondary follicles were cultured on UF-PLG-gel and gelatin scaffolds that were crosslinked with 1x or 2x concentrations of crosslinking reagent for 2, 4, or 6 days. Scaffold stiffness was measured by indentation testing (a,b). The area of attachment between follicles and scaffold struts was quantified for UF-PLG-gel (c) and gelatin (d)

scaffolds. Oocyte diameter was measured within intact follicles cultured on UF-PLG-gel (e) and gelatin (f) scaffolds. Graphs depict means ± SEM. Asterisks indicate significant differences between experimental groups. *P < 0.05, **P < 0.01, ***P < 0.001

Supplementary Files

This is a list of supplementary files associated with this preprint. Click to download.

- Supplementaryfigs.docx